

Ferromagnetism in zinc sulfide nanocrystals: Dependence on manganese concentration

I. Sarkar,¹ M. K. Sanyal,¹ S. Kar,² S. Biswas,² S. Banerjee,¹ S. Chaudhuri,² S. Takeyama,³ H. Mino,⁴ and F. Komori³

¹*Surface Physics Division, Saha Institute of Nuclear Physics, Kolkata 700 064, India*

²*Department of Material Science, Indian Association for the Cultivation of Science, Kolkata 700 032, India*

³*Institute for Solid State Physics, University of Tokyo, Chiba 277-8581, Japan*

⁴*Graduate School of Science and Technology, Chiba University, 1-33, Yayoi cho, Inage-ku, Chiba-shi, Chiba 263-8522, Japan*

(Received 1 April 2007; revised manuscript received 7 April 2007; published 8 June 2007)

Ferromagnetic ordering in nanocrystallites of dilute magnetic semiconductors arises due to a fascinating interplay of carrier concentration, randomness of magnetic impurity sites, and size-induced quantum confinement. We here report results of a magnetization study on ZnS nanoparticles (~ 2.5 nm) carried out by varying the doping concentration of substitutional Mn ions that occupy cationic sites without altering the carrier concentration. Ferromagnetic ordering and giant Zeeman splitting are observed below 30 K in these nanoparticles for doping above 1.5%. The change in coercive field ΔH_C exhibited \sqrt{T} temperature dependence expected for noninteracting nanoparticles. The values of blocking temperature T_B and H_C are found to be maximized for a doping level of 2.5% that corresponds to around five Mn atoms per ZnS nanocrystal.

DOI: 10.1103/PhysRevB.75.224409

PACS number(s): 75.75.+a, 71.55.Gs, 75.50.Pp

I. INTRODUCTION

Magnetic-ion-doped semiconductors popularly known as dilute magnetic semiconductors (DMSs) have been an active field of research due to their immense potential in spintronics applications.^{1,2} The difference between the two genre of DMS, namely, the group III-V (Refs. 3–5) and II-VI (Refs. 6 and 7) semiconductors, lies in the fact that the transition-metal impurities do not introduce additional charge carriers in II-VI semiconductors. This aspect is particularly interesting to refine our theoretical understanding of ferromagnetic ordering in DMS as proposed models^{8–11} depend strongly on both density of charge carriers and randomness of the magnetic impurity site. Yet another important facet in the magnetic ordering of DMS is the effect of dimensionality or confinement¹² as the hybridization of impurity d level with the valence band and conduction band of the host lattice plays a pivotal role in determining the type of interaction being mediated between the impurity sites.^{13,14} In spite of the myriad of intriguing effects^{15,16} expected in nanoparticles of DMS, only few systematic experimental studies^{17,18} have been carried out so far. Here, we report observation of ferromagnetism in 2.5 nm zinc sulfide nanoparticles having more than 1.5% manganese doping. The results on the magnetization study of 1.5%, 2.5%, 3.5%, and 6% Mn-doped 2.5 nm ZnS nanocrystals (NCs) are presented here that respectively corresponds to 3, 5, 7, and 12 Mn per NC,^{19,20} assuming that Mn ions occupy cationic sites. Earlier studies²⁰ on a similar system with low doping ($<1\%$) have shown them to be paramagnetic with signature of antiferromagnetic interaction. Our findings are quite intriguing as Mn doping in bulk ZnS does not exhibit ferromagnetism.^{21,22}

II. EXPERIMENTAL PROCEDURES

The Mn-doped ZnS nanocrystallites were prepared by solvothermal technique²³ by stirring together an appropriate amount of zinc acetate, manganese acetate, and thiourea in a Teflon-lined cell filled with ethanol up to 80% of its volume.

After stirring for 30 min, the reaction mixture was annealed at 433 K for 12 h and, finally, allowed to cool down naturally. The resulting white precipitate is filtered off and washed several times in water and ethanol. The transmission electron microscopy (TEM) measurements [Fig. 1(a)] show the particles to be highly crystalline and fairly monodisperse with an average size of 2.5 nm. The selected area electron diffraction pattern [inset Fig. 1(a)] confirms the crystallinity of the sample with lattice parameters consistent with zincblende phase of ZnS, revealing no perceivable lattice distortion. The sample was further characterized using x-ray photoelectron spectroscopy and energy dispersive x-ray analysis [Fig. 1(c)] to confirm the absence of any type of magnetic impurity except Mn. The positions and widths of the peaks in the powder x-ray diffraction data reconfirmed the zincblende structure and formation of 2.5 nm ZnS nanoparticles, respectively. Furthermore, photoluminescence (PL) measurement gave strong characteristic orange emission at room temperature associated with a transition between 4T₁ and 6A₁ energy levels of the Mn ions embedded in the ZnS lattice [Fig. 1(b)]. This confirmed that the Mn particles have preferentially gone to substitutional cationic sites inside the nanocrystals.²⁴

Magnetization measurements were carried out using a 7 T superconducting quantum interference device (MPMS Quantum Design) facility. The zero-field-cooled (ZFC) and field-cooled (FC) susceptibility (magnetization versus temperature) measurements were carried out respectively by cooling the sample in the absence and presence of field and by measuring the magnetization during the warming cycle. All the hysteresis measurements were performed by cooling the sample in zero field from 250 K. For field-cooled hysteresis measurements, samples were cooled in the presence of 5 T magnetic field. Samples having Mn concentration above 1.5% showed hysteresis [Fig. 1(e)], and detailed investigation presented below confirmed the existence of ferromagnetism in these ZnS nanocrystallites having 2.5%, 3.5%, and 6% Mn doping. The 1.5% doped sample showed paramagnetism down to 2 K.

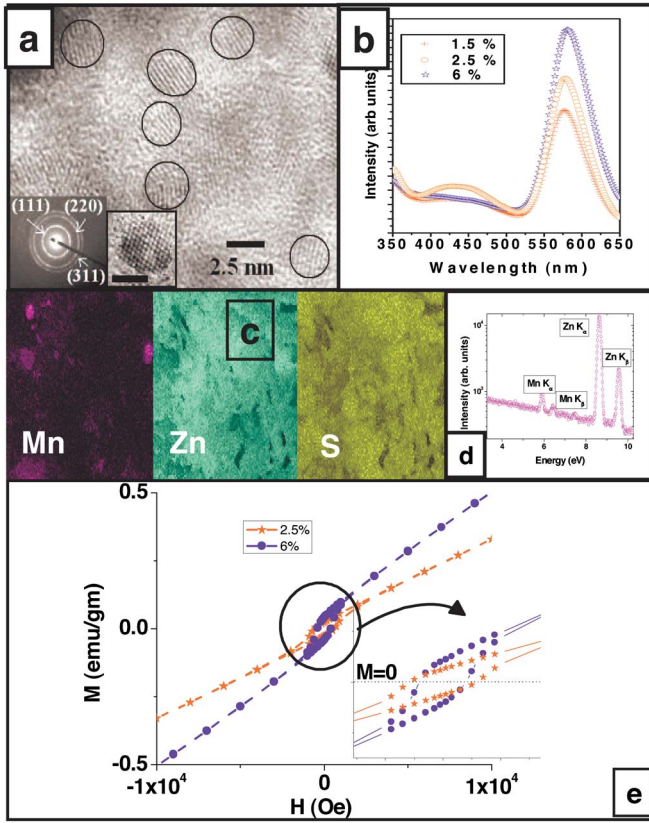


FIG. 1. (Color online) (a) TEM images of Mn-doped ZnS nanoparticles. (b) PL spectra of ZnS nanocrystals for different concentrations of Mn. (c) Elemental map for Mn-doped ZnS measured in scanning electron microscope showing the concentration of Mn, Zn, and S for the same area. (d) Energy dispersive x-ray analysis inclusive and exclusive of dashed region. No change is observed in relative intensities of Zn, Mn, and S in either case, indicating a marginal fraction of Mn precipitate in the sample. (e) Hysteresis plot of 2.5% and 6% Mn-doped ZnS at 10 K.

III. RESULTS AND DISCUSSIONS

The susceptibility plots [Fig. 2(a)] for 2.5%, 3.5%, and 6% doped samples clearly reveal a sharp branching in ZFC and FC data at low temperature that varies with concentration. No such branching was observed for 1.5% Mn doping within our measured temperature range. Such branching in the susceptibility plot is well known to occur in nanoparticle agglomerates,²⁵ signifying a blocking transition of individual nanoparticles from paramagnetic to an ordered state. The temperature at which this occurs is called blocking temperature, T_B . The existence of hysteric behavior with finite coercivity [Fig. 1(e)] below T_B clearly indicates that the Mn-doped ZnS nanoparticles undergo ferromagnetic transition below the blocking temperature T_B . Measurements were carried out to investigate the memory effect by cooling the sample in the presence and absence of field by stopping and waiting for 6 h at several temperatures below T_B , and then recording the magnetization while warming the sample. However, no change in magnetization was observed when no wait protocol was used. Absence of any memory effect in ZFC or FC magnetization measurements ruled out the tran-

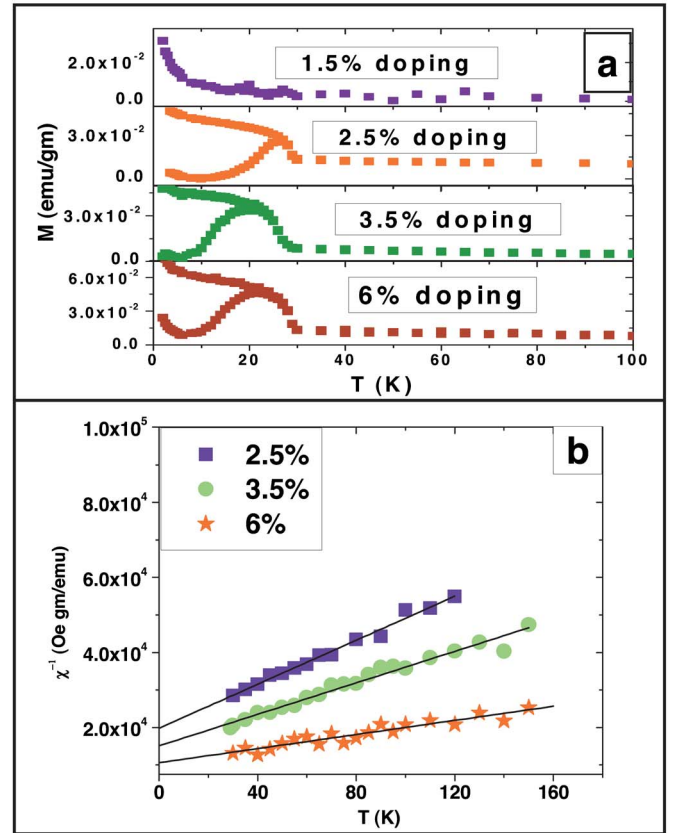


FIG. 2. (Color online) (a) ZFC-FC plot for different concentrations of Mn in ZnS at 300 Oe. (b) Inverse susceptibility plot for varying concentration of Mn along with Curie fit given by solid line.

sition to super-spin-glass state.^{26,27} The ac susceptibility measurements over a frequency range of 1–1000 Hz did not show any variation of T_B . This ruled out possible blocking due to superparamagnetic behavior of nanoparticles. The zero-field-cooled and field-cooled M vs H measurements showed no shift in hysteresis loop, ruling out the possibility of antiferromagnetic nanoparticles with net surface moments that may behave ferromagnetically.²⁸ The value of T_B that signifies ferromagnetic ordering is maximized for 2.5% doping (five Mn per NC) and takes the value of 28 K. For 3.5% and 6% doping, the corresponding values of T_B reduces to 21 and 20 K, respectively. The ferromagnetic ordering in 2.5% and higher concentration samples is further confirmed by the observation of thermal dependence in the change in coercive field $\Delta H_C(T) = [H_C(0) - H_C(T)]$ that follows a \sqrt{T} temperature dependence [Fig. 3(b)], $H_C(0)$ being coercive field at 0 K. Such temperature dependence is expected in a noninteracting ensemble of ferromagnetic particles^{18,29} and can be expressed as

$$H_C = H_C(0)[1 - (T/T_B)^{1/2}]. \quad (1)$$

$H_C(0)$, obtained by fitting Eq. (1), yields 0.295 and 0.23 T, respectively, for 2.5% doping and 6% doping. This result also shows that the 2.5% Mn-doped ZnS nanoparticles exhibit optimum ferromagnetism.

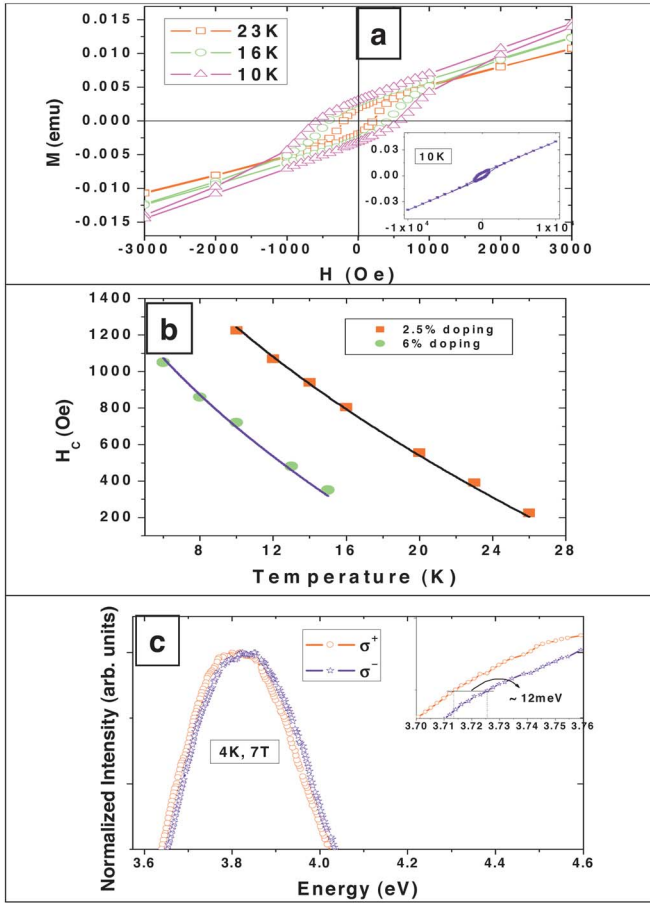


FIG. 3. (Color online) (a) Hysteresis plot of 2.5% Mn-doped ZnS at 10 K, 16 K, and 23 K. Inset shows nonsaturation behavior of magnetization even in the presence of hysteresis. (b) H_c vs T plot for 2.5% and 6% doping. The dashed line gives a fit to Eq. (1) to the data. Width of hysteresis has been taken as $H_c(T)$. (c) Spin-polarized PLE data for 2.5% doped sample measured at 4 K with 7 T field. The insets clearly show giant Zeeman splitting at 4 K.

Spin-polarized photoluminescence excitation (PLE) measurements were carried out by scanning a monochromator using Xe lamp as primary source. The data were collected in Faraday configuration with circularly polarized light and by changing the magnetic-field direction. A double monochromator was used to select the orange PL emission associated with a transition between 4T1 and 6A1 energy levels of the Mn ions embedded in the ZnS lattice. This spin-polarized PLE measurements gave an excitonic giant³⁰ Zeeman splitting ~ 12 meV at 7 T magnetic field below the transition temperature [Fig. 3(c)]. No such splitting was observed above T_B and for samples having doping below 2.5%. Such giant splitting is known to occur in DMS and requires the presence of strong exchange interaction between the Mn $3d$ states and the states of the semiconductor.³¹ This giant splitting is expressed as the sum of Zeeman splitting $\Delta E_g = g\mu_B H \sim 0.8$ meV and s - d exchange splitting.³² The observed value of ~ 12 meV clearly shows the presence of intrinsic exchange splitting³² leading to the formation of magnetic polaron,³³ thus evidencing the intrinsic origin of ferromagnetism.

The Curie-Weiss fit $\chi = C/(T - \theta)$ of high-temperature magnetization data [Fig. 2(b)] yields C Curie constant values of 1.08×10^{-3} , 1.616×10^{-3} , and 2.67×10^{-3} emu K Oe $^{-1}$ g m $^{-1}$, respectively, for 2.5%, 3.5%, and 6% Mn doping. This corresponds to an effective number of Bohr magneton values p of 5.82, 5.88, and 5.84, respectively. These values are close to the expected value of $p=5.9$ for Mn $^{2+}$, corresponding to a spin moment of $5/2$.³⁴ Furthermore, the fit gives θ values of -65 , -78 , and -113 K, respectively, for 2.5%, 3.5%, and 6%. This indicates enhancement of Mn-Mn antiferromagnetic interaction with higher doping due to the increase in Mn concentration. The II-VI DMS bound magnetic polaron (BMP) theory^{35,36} predicts that Mn spins can order antiferromagnetically with respect to the spins of carriers in the system. This can lead to a region of large magnetization, with all parallel polarized Mn spins, near the carrier leading to the formation of BMP. At sufficiently low temperatures, these BMPs can percolate through the system, resulting in long-range ferromagnetic order in the presence of antiferromagnetic interaction. However, with the enhancement of Mn doping, the theory predicts lowering of transition temperature due to enhanced antiferromagnetic interaction. This is consistent with the observed reduction in T_B with increase in Mn doping above 2.5%. This occurs due to a competition between the usual antiferromagnetic interaction mediated by virtual hopping of carriers and the loss of Mn $^{2+}$ carrier exchange energy by intermediate magnetic ions when the polaron moments are antiferromagnetically aligned.³⁵

The percolation theory of ferromagnetism based on BMP predicts that for three-dimensional systems, a small fraction ($\sim 20\%$) of Mn spins participate in percolation volume to settle in a ferromagnetic state.³⁶ The rest do not participate in ferromagnetism. These free spins align either at very high fields or at very low temperatures. Thus one expects a rise in magnetization both with the application of higher fields and at very low temperature, as has been confirmed through simulations.³⁶ The observation of a rise in magnetization at high field [inset Fig. 3(a)] and at temperature below 10 K in ZFC data [Fig. 2(a)], for 2.5%, 3.5%, and 6% samples, can thus be attributed to this phenomenon. Similar characteristic in magnetization has also been observed earlier in DMS (Refs. 37 and 38) systems. However, additional paramagnetic contribution of the marginal fraction of Mn atom that does not enter the NC, as indicated in Fig. 1(c), may also contribute to the rise in magnetization³⁹ below 10 K in ZFC data [Fig. 2(a)].

To test the veracity of the percolation model as a possible origin for ferromagnetism, an estimate of the effective percolation length R_{perc} was obtained for 2.5% doped nanoparticle using a ferromagnetic transition temperature expression based on percolation theory^{38,40} as follow: $K_B T_C = S(S+1)J(R_{perc})$, where T_C is the transition temperature, S is the spin of magnetic ion, and J is the distance-dependent exchange interaction. Assuming Bloembergen-Rowland-type interaction,⁴⁰

$$J(r) = -\frac{J_{pd}^2 m^2 \Delta}{\pi^3 \hbar^4 n^2 r^2} K_2(2r/r_0), \quad r_0 = \hbar(2m\Delta)^{-1/2}, \quad (2)$$

where n is the concentration of host atoms in the sublattice of substitution, m is the reduced electron mass, Δ is the smallest

excitation energy gap for electron, and $K_2(y)$ is the Macdonald function. Using $m=0.43m_0$, $\Delta=1.64$ eV, obtained from PL data using the relation $\Delta=E_g$ —peak emission energy⁴¹ for band gap $E_g=3.8$ eV for 2 nm ZnS nanoparticles, ferromagnetic exchange energy $J_{pd}=0.36$ eV for MnS,¹⁴ and $T_C=28$ K, we obtain $R_{perc}=0.4$ nm for a Mn spin moment of $S=5/2$. It is interesting to note that for a nanoparticle of ~ 2.5 nm with five Mn atom, the average inter-ion distance is ~ 0.5 nm, which is nearly equal to the percolation length obtained using the analysis. However, in contrast to the observed ferromagnetic optimization, this theory⁴⁰ predicts an increase in transition temperature T_C with increase in doping concentration because of a decrease in percolation length R_{perc} due to reduced interimpurity distance. This discrepancy arises as the mean-field calculation does not take into account the randomness of magnetic impurity, which has been theoretically shown to be the reason for the maximization of T_C (Ref. 11) for a specific impurity concentration in group III-V DMS.

IV. CONCLUSION

In conclusion, we have observed ferromagnetic ordering (above 1.5% doping) in Mn-doped 2.5 nm ZnS nanoparticles that is optimized at a 2.5% doping concentration of nanocrystals. The ferromagnetism is marked by the observation of blocking and hysteresis along with \sqrt{T} temperature dependence of the change in coercive field ΔH_C , which is known to occur for noninteracting ferromagnetic nanoparticles. We

have also observed giant Zeeman splitting of 12 meV at 7 T field that clearly indicates the intrinsic origin of ferromagnetism in these nanoparticles. Additionally, we observed nonsaturation of field dependence of magnetization along with low-temperature enhancement in magnetization. Such behavior may be explained based on percolation theory of BMP for ferromagnetism in DMS. However, these theories have been framed for bulk systems and it will be interesting to test the nuances of the model for these type of nano DMS systems. The disorder is expected to enhance ferromagnetic interaction in low-dimensional DMS.¹⁶ The intrinsic origin of ferromagnetism reported here may be due to movement of d level in the host lattice due to size reduction, which has been shown to be quite drastic for Mn-doped ZnS nanoparticles of size ~ 2 nm.⁴² It will be interesting to investigate the links between observed giant Zeeman splitting, possible magnetoelastic effect on zinc-blende structure at low temperature, and associated ferromagnetic ordering in ZnS nanoparticles. Hence the system reported here forms an ideal candidate to investigate the effects of confinement and randomness in impurity site on the ferromagnetic ordering in dilute magnetic semiconductors.

ACKNOWLEDGMENTS

The authors would like to thank Puru Jena for valuable discussions. Part of this work was supported by “Surface Interface Science (SIS)” subject group of India-Japan Cooperative Science Programme (IJCSF).

-
- ¹S. A. Wolf, D. D. Awschalom, R. A. Buhrman, J. M. Daughton, S. von Molnár, M. L. Roukes, A. Y. Chtchelkanova, and D. M. Treger, *Science* **294**, 1488 (2001).
- ²G. Prinz, *Science* **282**, 1660 (1998); I. Žutić, J. Fabian, and S. Das Sarma, *Rev. Mod. Phys.* **76**, 323 (2004).
- ³H. Ohno, *Science* **281**, 951 (1998).
- ⁴K. W. Edmonds, P. Boguslawski, K. Y. Wang, R. P. Campion, S. N. Novikov, N. R. S. Farley, B. L. Gallagher, C. T. Foxon, M. Sawicki, T. Dietl, M. Buongiorno Nardelli, and J. Bernholc, *Phys. Rev. Lett.* **92**, 037201 (2004); M. L. Reed, N. A. El-Masry, H. H. Stadelmaier, M. K. Ritums, M. J. Reed, C. A. Parker, J. C. Roberts, and S. M. Bedair, *Appl. Phys. Lett.* **79**, 3473 (2001).
- ⁵N. Theodoropoulou, A. F. Hebard, M. E. Overberg, C. R. Abernathy, S. J. Pearton, S. N. G. Chu, and R. G. Wilson, *Phys. Rev. Lett.* **89**, 107203 (2002).
- ⁶H. Saito, V. Zayets, S. Yamagata, and K. Ando, *Phys. Rev. Lett.* **90**, 207202 (2003).
- ⁷P. Sharma, A. Gupta, K. V. Rao, F. J. Owens, R. Sharma, R. Ahuja, J. M. Osorio Guillen, B. Johansson, and G. A. Gehring, *Nat. Mater.* **2**, 673 (2003); M. Venkatesan, C. B. Fitzgerald, J. G. Lunney, and J. M. D. Coey, *Phys. Rev. Lett.* **93**, 177206 (2004).
- ⁸L. Bergqvist, O. Eriksson, J. Kudrnovský, V. Drchal, P. Korzhavyi, and I. Turek, *Phys. Rev. Lett.* **93**, 137202 (2004); A. Kaminski and S. Das Sarma, *ibid.* **88**, 247202 (2002).
- ⁹T. Dietl, H. Ohno, F. Matsukura, J. Cibert, and D. Ferrand, *Science* **287**, 1019 (2000); J. König, H. H. Lin, and A. H. MacDonald, *Phys. Rev. Lett.* **84**, 5628 (2000).
- ¹⁰C. Timm, *Phys. Rev. Lett.* **96**, 117201 (2006); M. Berciu and R. N. Bhatt, *ibid.* **87**, 107203 (2001).
- ¹¹A. Kaminski, V. M. Galitski, and S. Das Sarma, *Phys. Rev. B* **70**, 115216 (2004); D. J. Priour, Jr. and S. Das Sarma, *ibid.* **73**, 165203 (2006).
- ¹²X. Huang, A. Makmal, J. R. Chelikowsky, and L. Kronik, *Phys. Rev. Lett.* **94**, 236801 (2005).
- ¹³P. Kacman, *Semicond. Sci. Technol.* **16**, R25 (2001).
- ¹⁴B. E. Larson, K. C. Hass, H. Ehrenreich, and A. E. Carlsson, *Phys. Rev. B* **37**, 4137 (1988); J. K. Furdyna, *J. Appl. Phys.* **64**, R29 (1988).
- ¹⁵S. Sapra, D. D. Sarma, S. Sanvito, and N. A. Hill, *Nano Lett.* **2**, 605 (2002).
- ¹⁶T. Dietl, A. Haury, and Y. M. d’Aubigné, *Phys. Rev. B* **55**, R3347 (1997).
- ¹⁷T. Meron and G. Markovich, *J. Phys. Chem. B* **109**, 20232 (2005); J. Luo, J. K. Liang, Q. L. Liu, F. S. Liu, Y. Zhang, B. J. Sun, and G. H. Raoy, *J. Appl. Phys.* **97**, 086106 (2005); B. Martínez, F. Sandiumenge, L. Balcells, J. Arbiol, F. Sibieude, and C. Monty, *Phys. Rev. B* **72**, 165202 (2005).
- ¹⁸P. Poddar, Y. Sahoo, H. Srikanth, and P. N. Prasad, *Appl. Phys. Lett.* **87**, 062506 (2005); K. M. Hanif, R. W. Meulenberg, and G. F. Strouse, *J. Am. Chem. Soc.* **124**, 11495 (2005).

- ¹⁹P. E. Lippens and M. Lannoo, Phys. Rev. B **39**, 10935 (1989).
- ²⁰N. Tsujii, H. Kitazawa, and G. Kido, J. Appl. Phys. **93**, 6957 (2003); J. Schrier and K. B. Whaley, *ibid.* **95**, 1436 (2004); Y. Wang, N. Herron, K. Moller, and T. Bein, Solid State Commun. **77**, 33 (1991).
- ²¹K. Sato and H. K. Yoshida, Phys. Status Solidi B **229**, 673 (2002).
- ²²V. Bindilatti, E. ter Haar, N. F. Oliveira, Y. Shapira, and M. T. Liu, Phys. Rev. Lett. **80**, 5425 (1998).
- ²³S. Biswas, S. Kar, and S. Chaudhuri, J. Phys. Chem. B **109**, 17526 (2005).
- ²⁴K. Sooklal, B. S. Cullum, S. M. Angel, and C. J. Murphy, J. Phys. Chem. **100**, 4551 (1996); R. N. Bhargava, D. Gallagher, X. Hong, and A. Nurmikko, Phys. Rev. Lett. **72**, 416 (1994).
- ²⁵A. Aharoni, *Introduction to theory of Ferromagnetism* (Oxford University Press, Oxford, 2000).
- ²⁶Y. Sun, M. B. Salamon, K. Garnier, and R. S. Averback, Phys. Rev. Lett. **91**, 167206 (2003); J. L. Dormann, R. Cherkaoui, L. Spinu, M. Nogués, F. Lucari, F. D'Orazio, D. Fiorani, A. Garcia, E. Tronc, and J. P. Jolivet, J. Magn. Magn. Mater. **187**, L139 (1998); C. Djurberg, P. Svedlindh, P. Nordblad, M. F. Hansen, F. Bodker, and S. Morup, Phys. Rev. Lett. **79**, 5154 (1997).
- ²⁷M. Sasaki, P. E. Jönsson, H. Takayama, and H. Mamiya, Phys. Rev. B **71**, 104405 (2005).
- ²⁸M. Gruyters, Phys. Rev. Lett. **95**, 077204 (2005).
- ²⁹F. C. Fonseca, G. F. Goya, R. F. Jardim, R. Muccillo, N. L. V. Carreño, E. Longo, and E. R. Leite, Phys. Rev. B **66**, 104406 (2002).
- ³⁰V. V. Rossin, J. Puls, and F. Henneberger, Phys. Rev. B **51**, 11209 (1995).
- ³¹L. M. Sandratskii, Phys. Rev. B **68**, 224432 (2003).
- ³²R. C. Myers, M. Poggio, N. P. Stern, A. C. Gossard, and D. D. Awschalom, Phys. Rev. Lett. **95**, 017204 (2005).
- ³³K. Yanata, K. Suzuki, and Y. Oka, J. Appl. Phys. **73**, 4595 (1993); A. K. Bhattacharjee and C. Benoit à la Guillaume, Phys. Rev. B **55**, 10613 (1997).
- ³⁴C. Kittel, *Introduction to Solid State Physics* (Wiley, New York, 2003).
- ³⁵P. A. Wolff, R. N. Bhatt, and A. C. Durst, J. Appl. Phys. **79**, 5196 (1996).
- ³⁶R. N. Bhatt, M. Berciu, M. P. Kennett, and X. Wan, J. Supercond. **15**, 71 (2002).
- ³⁷H. Hori, S. Sonoda, T. Sasaki, Y. Yamamoto, S. Shimizu, K. Suga, and K. Kindo, Physica B **324**, 142 (2007).
- ³⁸Y. D. Park, A. T. Hanbicki, S. C. Erwin, C. S. Hellberg, J. M. Sullivan, J. E. Mattson, T. F. Ambrose, A. Wilson, G. Spanos, and B. T. Jonker, Science **295**, 651 (2002).
- ³⁹X. Chen, S. Bedanta, O. Petracic, W. Kleemann, S. Sahoo, S. Cardoso, and P. P. Freitas, Phys. Rev. B **72**, 214436 (2005).
- ⁴⁰V. I. Litvinov and V. K. Dugaev, Phys. Rev. Lett. **86**, 5593 (2001).
- ⁴¹W. Schairer and M. Schmidt, Phys. Rev. B **10**, 2501 (1974).
- ⁴²V. Albe, C. Jouanin, and D. Bertho, Phys. Rev. B **57**, 8778 (1998).